Letters

Predicting Function from Structure Using the Poisson−Nernst−Planck Equations: Sodium Current in the Gramicidin A Channel

Uwe Hollerbach

Department of Molecular Biophysics & Physiology, Rush Medical College, Chicago, Illinois 60612

Duan P. Chen*

Department of Molecular Biophysics & Physiology, Rush Medical College, Chicago, Illinois 60612

David D. Busath

Department of Zoology, Brigham Young University, Provo, Utah 84602

Bob Eisenberg

Department of Molecular Biophysics & Physiology, Rush Medical College, Chicago, Illinois 60612

We predict the sodium current through an ion channel of known structure—gramicidin A (gA)—using an electrostatic model of the ion channel and an electrodiffusion model of ion movement. We use three-dimensional (3D) spectral elements to represent the channel and macroscopic surrounding baths in a 3D Poisson−Nernst−Planck (PNP) calculation that uses fine resolution only where needed in the channel pore region. Diffusion coefficient and dielectric constants are estimated from a 1D PNP representation of the experimental data. The 3D atomic structure and standard empirical partial charges of gA are used, along with the diffusion coefficients estimated from 1D PNP. No adjustable parameters were used in the 3D PNP calculation. No attempts were made to improve fit by adjusting parameters. Our results show that 3D PNP is an accurate description of charge transport in this channel system and thus a good place to start investigation of other channels. We predict unreported experiments as a further test of the theory.

Introduction

Transport properties of biological ionic channels are difficult to calculate from their atomic structure, because they span macroscopic and atomic length scales and a time scale ranging over orders of magnitude as well. Computing the macroscopic properties of a large biological system with atomic details is impractical and may not yield insight, even if feasible. Computing the system only

* To whom correspondence may be addressed. E-mail: dchen@rush.edu. http://144.74.27.66/reprint.html.

on the atomic scale is likely to mislead, because macroscopic features of the system provide the sources of energy and matter that keep the system away from equilibrium. Most biological systems, especially transport proteins, only work when they are far from equilibrium. Here we compute the function of a system of considerable biological importance, ionic channels, in atomic detail using an electrostatic model of the channel and an electrodiffusion model of ion movement. The well-known mathematical technique of spectral elements of multiresolution in space provides a practical approach to this channel system because computation is focused on the channel region where atomic detail is needed.

Ionic channels, found in lipid membranes of living cells, control the rapid passage of ions and the resulting current of charge. Ionic current is used throughout living systems to perform key physiological functions, for example, signaling in the nervous system, signal transduction in sensory organs, and coordination of muscle contraction. Channels help control transport in nearly every tissue and cell.[1]

Gramicidin A is a model ionic channel, which forms an aqueous pore of 2 Å in radius and 25 Å in length across a lipid membrane. It is a hydrophobic linear polypeptide, formed by spontaneous dimerization of monomers into the lipid bilayer, making a cation selective pathway. (Anions do not permeate.) Each monomer of gramicidin is composed of 15 amino acids alternating (nearly always) between L and D stereoisomers, L-VAL-GLY-L-ALA-D-LEU-L-ALA-D-VAL-L-VAL-D-VAL-L-TRP-D-LEU-L-TRP-D-LEU-L-TRP-D-LEU-L-TRP. Because of its simplicity, gA is well-studied both experimentally and theoretically.[2−4]

In the past, the permeation of ions across biological cell membranes has been described by the constant-field theory of Goldman, Hodgkin, and Katz (GHK)[5,6] or by an exponential theory of hopping over barriers reminiscent of Eyring rate theory.[7,8] Many efforts have been made to predict gramicidin currents based on these two types of models.[9] From both approaches, it appears that entry into the channel is rate limiting when the channel is unoccupied, exit is rate limiting (rather than translocation) when the channel is singly occupied, but translocation is rate limiting when the channel is doubly occupied. If an arbitrary energy profile is built into GHK or Eyring models, and a prefactor different from the Kramers prefactor[10] is used, many data sets can be fit; however, using arbitrary energy profiles without structural correlates is unsatisfying when a real channel structure is available. The apparent energy profiles are not easily correlated to the structure of the channel, for example, to the locations of its partial charges, or to the long-range electrostatic/electrodiffusion forces of the transmembrane potential that keep the system working, away from equilibrium.

Poisson−Nernst−Planck (PNP) and the present 3D PNP calculations show that the potential profile for ion permeation is not constant at all. The energy profile is a sensitive function of ionic concentration in the bath and depends nonlinearly on the applied transmembrane potential. Furthermore, the self-consistently calculated potential profile very likely does not have a single high barrier. Therefore, the usefulness of old theories (constant-field theory and Eyring rate theory) is rather limited for ion channel permeation.[11]

Here, we use the well-known mathematical method of spectral elements to perform a three-dimensional electrostatic calculation of the structurally well-defined gramicidin A (gA) channel.[12,13] The electrostatics of the protein and electrodiffusion of ions is described by the PNP equations.[14] Reaching beyond the GHK/Nernst−Planck formulation, PNP includes the effects of permeating ions on the electric field, on the induced charge at dielectric boundaries, and on interionic interactions mediated by the mean field. PNP is the natural extension of the (nonlinear) Poisson−Boltzmann theory[15−17] to nonequilibrium systems to predict currents and other transport properties.

In PNP, the charge distribution in the channel protein is used explicitly to determine the electrochemical potential energy profile encountered by the permeating ion in either a 1D or 3D paradigm. In 3D PNP, the structure is represented by the positions and values of the partial charges of the atoms of its independently known structure. The latter form of the theory has recently been developed in ref 18 and is implemented here with spectral elements. In the 1D version of PNP, structural parameters are determined by a fitting procedure described previously.[19,20] The charge distribution along a channel protein (in this paper, gA) is assumed to be axially symmetric and is represented by 10 parametric bins. A full account of the 1D PNP fit for gA will be reported elsewhere. 1D PNP is used in the present paper only to estimate the values of the diffusion coefficient for Na^+ and Cl^- and the dielectric constant inside the gA pore. The charge distribution determined by 1D PNP is not used in the present paper.

Method

Our starting point is the published structure of gA (coded 1MAG in the Brookhaven Protein Data Bank, as measured by solid-state NMR and refined with the contribution from the CHARMM force-field:[13] Figure 1). A mesh of finite elements, the spectral elements, represent the structure, the lipid, and the baths (Figure 2). Small elements are used in the channel and large elements in the baths. The charge distribution of the channel (each atom or entire chemical group) is assigned by the scheme in OPLS (a force field widely used to simulate molecular dynamics of protein molecules[21]). The charge distribution on the lipid is assumed to be zero. The dielectric constant is assigned to a fixed value throughout the entire space in our calculation: the regions in space occupied by lipid and gA are assigned to have a value of 2 (even though the charge

(1) Ashcroft, F. M. *Ion Channels and Disease*; Academic Press: New York, 1999.
(2) Andresen, O. S.; Koeppe, R. E., II *Physiol. Rev.* **1992**, *72*, S89.
(3) Jordan, P. C. *J. Phys. Chem.* **1991**, *91*, 6582.
(4) Roux, B. *Biophys. J.* **1999**, *77*, 139.
(5) Goldman, D. E. *J. Gen. Physiol.* **1943**, *27*, 37.
(6) Hodgkin, A. L.; Katz, B. *J. Gen. Physiol.* **1949**, *108*, 37.
(7) Hille, B.; Schwarz, W. *J. Gen. Physiol.* **1978**, *72*, 409.
(8) Nonner, W.; Chen, D. P.; Eisenberg, B. *J. Gen. Physiol.* **1999**, *113*, 773.
(9) Busath, D. D. *Annu. Rev. Physiol.* **1993**, *55*, 473 and references therein.
(10) Hänggi, P.; Talkner, P.; Borokovec, M. *Rev. Mod. Phys.* **1990**, *62*, 251.

(11) Chen, D. P.; Eisenberg, R. S. *Biophys. J.* **1993**, *64*, 1405.
(12) Arseniev, A. S.; Lomize, A. L.; Barsukov, I. L.; Bystrov, V. F. *Biol. Membr.* **1990**, *3*, 1723.
(13) Ketchum, R. R.; Roux, B.; Cross, T. A. *Structure* **1997**, *5*, 1655.
(14) Eisenberg, B. *Acc. Chem. Res.* **1998**, *31*, 117.
(15) Honig, B.; Nichols, A. *Science* **1995**, *268*, 1144.
(16) Davis, M. E.; McCammon, J. A. *Chem. Rev.* **1990**, *90*, 509.
(17) Forsten, K. E.; Kozack, R. E.; Lauffenburger, D. A.; Subramaniam, S. *J. Phys. Chem.* **1994**, *98*, 5580.
(18) Kurnikova, M. G.; Coalson, R. D.; Graf, P.; Nitzan, A. *Biophys. J.* **1999**, *76*, 642.
(19) Chen, D. P.; Xu, L.; Tripathy, A.; Meissner, G.; Eisenberg, B. *Biophys. J.* **1997**, *73*, 1337.
(20) Chen, D. P.; Xu, L.; Tripathy, A.; Meissner, G.; Eisenberg, B. *Biophys. J.* **1999**, *76*, 1346.
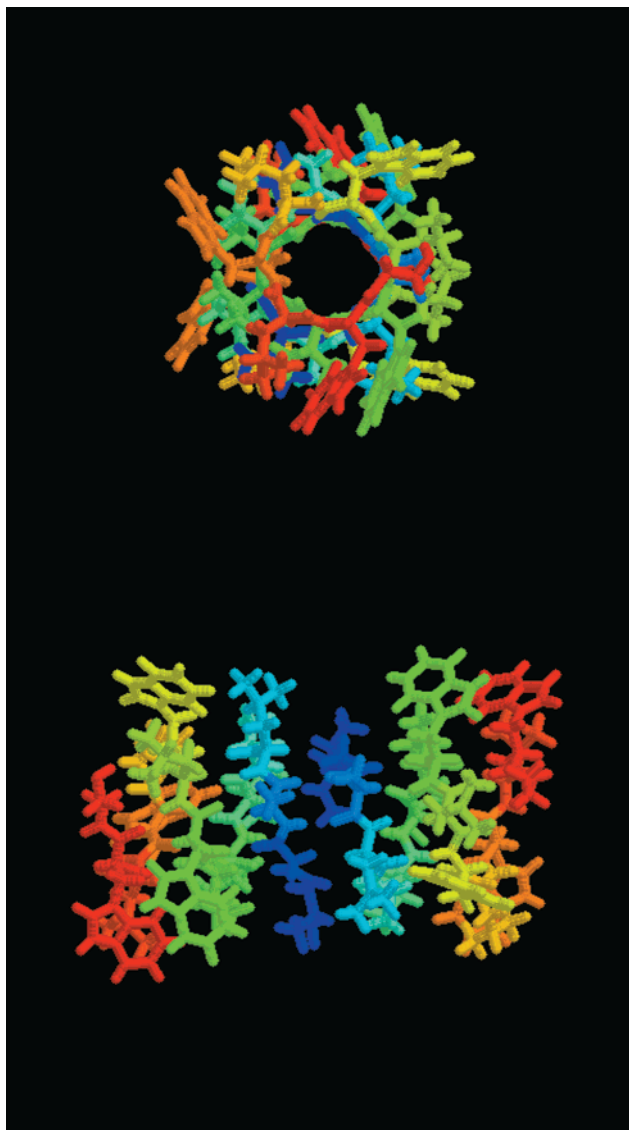(21) Jorgensen, W. L.; Tirado-Rives, J. *J. Am. Chem. Soc.* **1988**, *110*, 1666.

Figure 1. The gA dimer structure (PDB structure 1MAG). Top picture is the view through the gA channel and lower picture is the side view. The channel has an internal diameter of 4 Å and a length of 25 Å. Amino acids are colored by residue number from the N terminal (blue) to the C terminal (red), demonstrating the channel symmetry resulting from head-to-head dimerization.

distribution is not zero where gA is); the bath and the pore region to a fixed dielectric constant of 80. Water molecules are not treated explicitly, but as a continuum of a dielectric constant 80. The pore region is assumed to be aqueous; therefore it takes a dielectric constant of 80. We have found the bulk value of dielectric constant is the best value in our 1D PNP least-squares fit to the same data. The diffusion coefficients are assigned to the value determined by 1D PNP least-squares fit, and no attempt is made to vary them to fit the data better in 3D PNP calculation. Specifically, the diffusion coefficient for sodium ions is $D(Na^+) = 4.67 \times 10^{-7}$, and for chloride ions $D(Cl^-) \simeq 1.0 \times 10^{-8}$ cm²/s.

The OPLS charge distribution, diffusion, and dielectric constants are the inputs to 3D PNP, without adjustable parameters. We simply compute the current−voltage (*I*−*V*) relations expected in a given experimental condition by successively integrating the coupled Poisson and Nernst−Planck equations in a Gummel iteration. An initial guess of the profile of electrical potential is used to compute a congruent initial guess of the ion concentra-

tion profiles using the Nernst−Planck equation that describes the probability of location of an ion. These "concentration" profiles are then substituted back into the Poisson equation to update the electrical potential. This back-and-forth Gummel iteration[22] is continued until the solutions to the individual equations have converged to a self-consistent overall solution. The PNP equation reads:

$$
\begin{cases}
-\nabla\cdot(\epsilon_{a,m}\nabla\Psi) = \sum_j z_j e C_j(x,y,z) + P(x,y,z), \\
J_j = -D_j[\nabla C_j(z) + z_j e C_j(z)\nabla\Psi(z)], & \text{for } j = 1 \ldots N, \\
C_j(x,y,0) = C_j(L), & \text{for } j = 1 \ldots N, \text{ at } z = 0, \\
\Psi(x,y,0) = 0, \\
C_j(x,y,d) = C_j(R), & \text{for } j = 1 \ldots N, \text{ at } z = d, \\
\Psi(x,y,d) = V_{appl},
\end{cases}
\tag{1}
$$

where d the length of the box in our calculation, $P(x,y,z)$ is the charge distribution of the channel protein according to the scheme in OPLS, $C_j(L)$ is the concentration in the left bath; $C_j(R)$ is the concentration in the right bath, ϵ_a is the dielectric constant of the aqueous pore, ϵ_m is the dielectric constant in the region of lipid and the channel protein (where $P(x,y,z) = 0$, and $C_j(x,y,z) = 0$), and V_{appl} is the applied voltage. The electric current is then $I = \sum_i e z_i J_i(z) A(z)$, where A is the channel cross-sectional area. In addition, we assume $\Psi = 0$ and no flux boundary condition in all the surface of the box except two planes at $z = 0$ and $z = d$.

The individual equations are solved using the spectral element method, a finite-element method[23,24] of Galerkin type that uses high-order orthogonal polynomials as basis functions.[25,26] The spectral elements discretize the partial differential equations into a system of linear algebraic equations, which (in our case) are conveniently solved using the conjugate-gradient method.[27,28] The spectral elements provide a nonuniform mesh that focuses computation efficiently, on the channel not the bath.

One weakness of this approach which has been criticized[29] and deserves attention is that solvent and ions in the pore are simulated by dielectric continuum and probability density rather than explicitly, so interactions may not be realistic in multiple occupancy situation. However, a direct comparison of experimental *I*−*V* with calculation will provide a stringent test of the practical significance of this criticism.

The data selected for fitting were taken from ref 30. It consists of *I*−*V* relations for gramicidin A channels in planar lipid bilayers formed with DPhPC in decane (20 mg/mL). It should be noted that the currents measured in a different type of lipid (glyceryl monoolein) differed

(22) Jerome, J. W. *Analysis of Charge Transport: A Mathematical Study of Semiconductors*; Springer-Verlag: Heidelberg, 1996.

(23) Strang, G.; Fix, G. J. *An Analysis of the Finite Element Method*; Prentice Hall series in automatic computation; Prentice Hall: Englewood Cliffs, NJ, 1973.

(24) Zienkiewicz, O. C. *The Finite Element Method in Engineering Science*, 2nd ed.; McGraw-Hill: New York, 1971.

(25) Patera, A. T. *J. Comput. Phys.* **1984**, *54*, 468.

(26) Ghaddar, N. K.; Karniadakis, G. E.; Patera, A. T. *Numer. Heat Transfer* **1986**, *9*, 227.

(27) Hestenes, M.; Stiefel, E. *J. Res. Natl. Bur. Stand.* **1952**, *49*, 409.

(28) Press, W. H.; Teukolsky, S. A.; Vetterling, W. T.; Flannery, B. P. *Numerical Recipes: the Art of Scientific Computing*, 2nd ed.; Cambridge University Press: New York, 1992.

(29) Dieckmann, G. R.; Lear, J. D.; Zhong, Q.; Klein, M.; DeGrado, W.; Sharp, K. A. *Biophys. J.* **1999**, *76*, 618.

(30) Busath, D. D.; Thulin, C. D.; Hendershot, R. W.; Phillips, L. R.; Maughan, P.; Cole, C. D.; Bingham, N. C.; Morrison, S.; Baird, L. C.; Hendershot, R. J.; Cotten, M.; Cross, T. A. *Biophys. J.* **1998**, *75*, 2830.
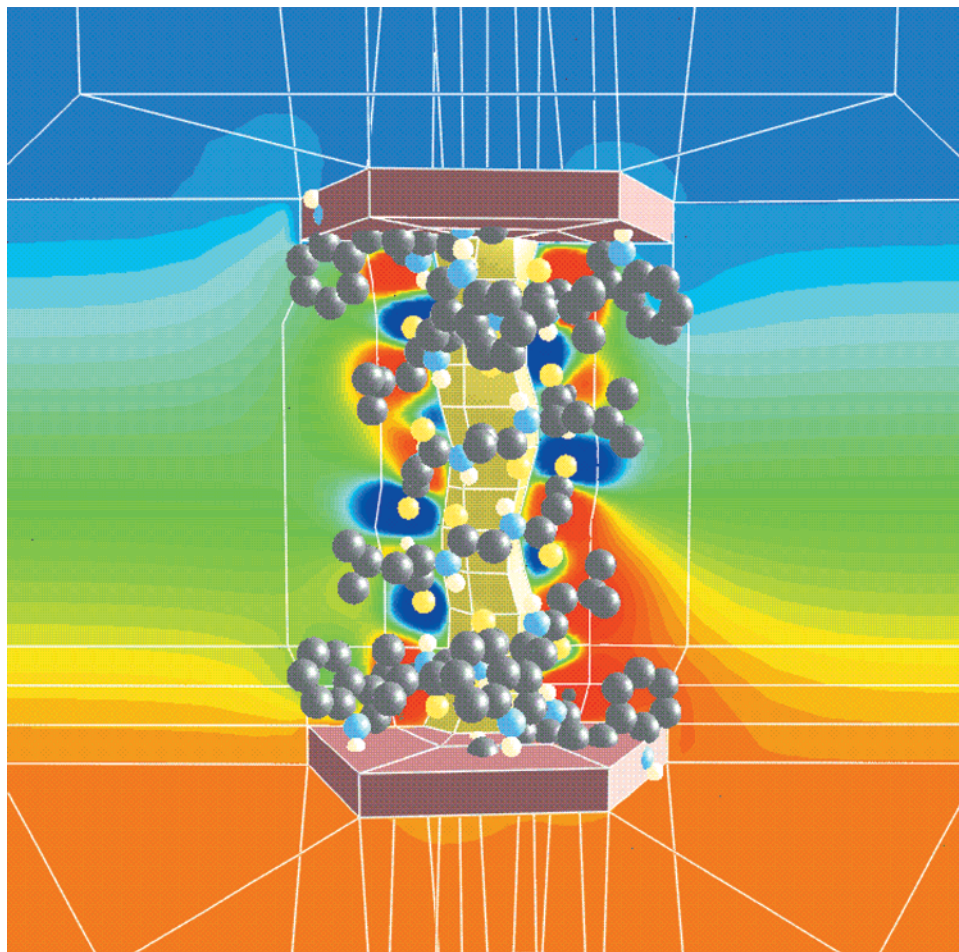
Figure 2. A schematic view of the central portion of the geometry used to solve the Poisson−Nernst−Planck (PNP) equations for the gramicidin A channel. The channel is vertical in this picture. The yellow elements represent the actual hole through the gramicidin dimer. Only the backbone and those atoms of the gramicidin dimer which have nonzero charge are shown: carbon in black, nitrogen in blue, oxygen in yellow, and hydrogen in off-white. The reddish-brown regions at the ends of the dimer represent "atrium" regions. In this computation the "atrium" regions have the same properties as the bulk of the bath, which extends above and below the channel. The upper bath is essentially the three-dimensional extension of the solid medium-blue region at the top of the figure, and the lower bath is the extension of the solid orange region at the bottom. The lipid bilayer is represented as an impermeable region surrounding the channel and located between the two horizontal planes forming the outer borders of the "atrium" regions. The atomic character of the lipid molecules is not taken into account in this simulation. The white lines show the edges of some of the spectral elements. Each spectral element contains nearly a thousand basis functions, which are combinations of high-order Legendre polynomials. The use of spectral elements allows extremely accurate calculation of the solutions to the PNP equations. The color contour plot shows a cross section, extending through the center of the channel, of the electrical potential (the contours inside the channel are hidden by the channel elements). Red indicates regions of high potential, and blue indicates low potential. In this computation, the applied potential is +0 mV at the top (medium-blue) of the image and +200 mV at the bottom (orange). The potentials inside the molecule are significantly larger in magnitude than the applied potential, ranging from −870 to +930 mV (as indicated by the more-saturated blue and red, respectively), and regions of positive and negative potential spiral around the central axis of the channel exactly following the backbone of the gramicidin molecules. It is clear from the image that the internally generated electric fields dominate and that the applied bath voltage causes only a relatively small perturbation of those internal electric fields. A symmetric 100 mM NaCl ionic condition is used in the calculation.

from those used here. Future work with 3D PNP will address the effect of the interfacial dipole potential on the currents, but no provisions were made for the lipid electrostatics in the computations presented here.

Result and Discussion

The data and the prediction of the 3D PNP calculation are shown in Figure 3. NaCl concentrations are the same on both sides of the bilayer, and the gA channel is symmetrical as are measured current−voltage relations, so only one limb of the $I-V$ relation need be shown. The solid lines are the predictions of 3D PNP, and the symbols are measured currents. Agreements in shape and magnitude are very good (except in the 0.1 M salt), considering that all parameters were preset: no fitting was performed.

Our calculations show that $I-V$ values are slightly superlinear (within physiological ionic strength), because the increase in the applied voltage not only increases the net driving force but also increases the sodium ion occupancy inside the channel. An higher applied voltage has a similar effect to increase the ionic strength in the baths, shown in Figure 4.

The disagreement of this calculation with experiment could be attributed to the fact that the lipid is not explicitly included in the present calculation, whereas it is known that the lipid can affect the $I-V$ significantly. Another possibility is that activities not concentrations are used in the calculation as the concentration boundary conditions. We do not have any reason to believe that the activity coefficients in the bulk could extend inside the gA channel pore. Since water molecules are not modeled explicitly either, the ignored hydration/dehydration energy could change the calculated $I-V$ values.

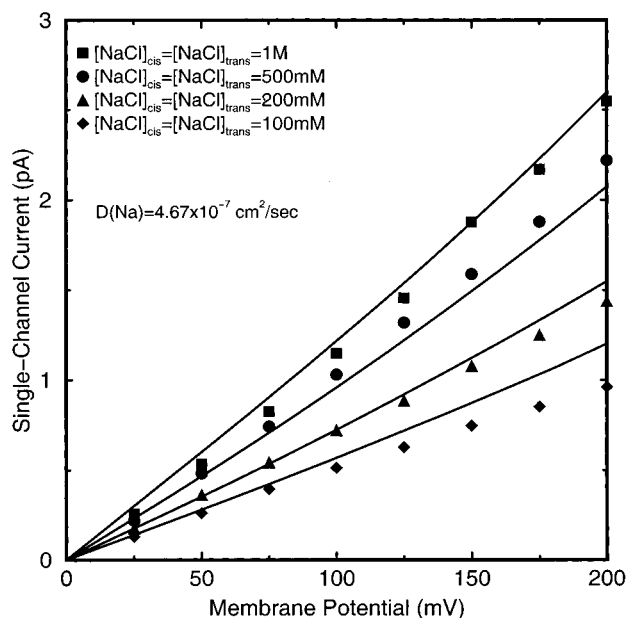Figure 4 shows the predicted occupancy of the channel

Figure 3. Predicted current−voltage relations from the 3D-PNP calculation for various symmetric NaCl salt solutions of gramicidin A channel in DPhPC lipid. The solid lines of different colors are from the theoretical PNP calculation, and the symbols (indicating different salt concentrations) are experimental points. In the 3D PNP calculation, there is NO free parameter: diffusion coefficients are from 1D PNP least-squares fit, and the charge distributions are from the AMBER force field of molecular dynamics simulation. Symbols are approximately 2 SEM in height.
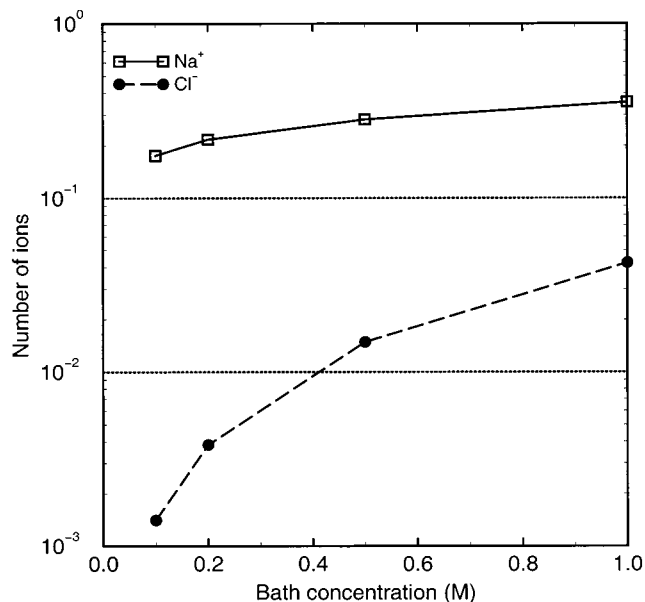

Figure 4. Calculated occupancies of sodium ions and chloride ions in the pore of a gramicidin A channel. The calculations are done with a holding potential of 60 mV for various symmetric salt concentrations. The open squares are for sodium ions, showing nearly constant occupancy. The filled circles are for chloride ions, and their values are predicted to be 1 or 2 orders of magnitude lower than the more permeant sodium ions.

by Na^+ and Cl^- at different concentrations when 60 mV is applied across the bilayer. The occupancy is the integral of the Na^+ concentration over the pore region. The occupancy changes little over the range of holding potentials, because the contents of the open channel are buffered by its effective fixed charge, as we have described in previous publications;[20] however, the Na^+ occupancy is less than that expected from the gramicidin the litera-

ture.[31,32] Cl^- is excluded from the channel even though the protein is electroneutral overall. The spatial distribution of atomic charge is nonuniform in the channel protein, and the resulting negativity in the channel's pore excludes anions, consistent with the historical literature.[33] This fact, combined with its low value of diffusion coefficient, makes the Cl^- contribution to current negligible.

The quantitative success of this simple electrostatic/electrodiffusion description in predicting the gA channel current is striking. However, the predicted occupancies are rather low. The model predicts that channel occupancy is only 0.37 at 1 M salt, indicating that the binding affinity is <1 M^{-1}. Experimental estimates of the gA binding affinity for a single Na^+ range from 1.43 to 100 M^{-1}, depending on the method of determination and lipid used.[34] Tl205 NMR competition studies yield 36.9 M^{-1} in lyso-lecithin micelles[34] and water permeability inhibition in planar glyceryl monoolein bilayers suggests 12.5 M^{-1},[35] whereas kinetic models of $I-V$ relations generally yield values of 3−4 M^{-1}. Therefore, our predicted occupancies are lower than that which would be predicted even by the lowest binding affinities previously obtained. On the other hand, our predictions are consistent with the common assertion that double occupancy is unlikely in gA for Na^+,[32] even though many lines of evidence indicate that double occupancy is prevalent for the larger alkali metal cations. Thus, complications due to inadequate treatment of double occupancy do not confound the current computations presented here.

The sensitivity of our calculation to parameters in PNP theory was evaluated in several ways. First, consider the diffusion constant of chloride ions $D(Cl^-)$, which is hard to estimate reliably in gA (as in other cation channels we have studied[20]), because chloride is strongly electrostatically excluded from the pore and thus carries immeasurable current. The prediction of electrical current in both 1D and 3D PNP is insensitive to the value of $D(Cl^-)$ if $D(Cl^-) < D(Na^+)$. Specifically, at a potential of 180 mV in 1 M symmetrical NaCl, the current is 2.7 pA for negligible $D(Cl^-) \simeq 1.0 \times 10^{-8}$ cm^2/s, compared to 2.8 pA if $D(Cl^-) = 1.0 \times 10^{-6}$ cm^2/s, due to the reduced occupancy for electrostatic reasons. In 1D systems, we can show analytically that the occupancy of the channel by co-ions (i.e., Cl^-) is strictly independent of the value of $D(Cl^-)$: For a given holding membrane potential, it only depends on the fixed charge distribution on the channel. However, the calculated electrical current is proportional to the diffusion coefficient of sodium ions, though we do not attempt to vary it to achieve better fit. The value used in the calculation is $D(Na^+) = 4.67 \times 10^{-7}$.

The calculated electric current depends monotonically but weakly on the dielectric constants chosen to describe the lipid−protein, bath, and pore. The dielectric constant in the baths has virtually no effect on the calculated current. The lipid is described by a dielectric constant of 2. As the dielectric constant of the lipid is increased from $2 \rightarrow (4) \rightarrow 6$, the calculated current increases by only 6%. The pore region is described by a dielectric constant of 80, because smaller values will not fit the data, using either 1D or 3D PNP. As the dielectric constant in the pore is increased from $40 \rightarrow 80$, the net current increases from

(31) Jing, N.; Prasad, K. U.; Urry, D. W. *Biochim. Biophys. Acta* **1995**, *1238*, 1.
(32) Heinemann, S. H.; Sigworth, F. J. *Biochim. Biophys. Acta* **1989**, *987*, 8.
(33) Roux, B. *Biophys. J.* **1996**, *71*, 3177.
(34) Hinton, J. F.; Whaley, W. L.; Shungu, D.; Koeppe, R. E., II; Millett, F. S. *Biophys. J.* **1986**, *50*, 539.
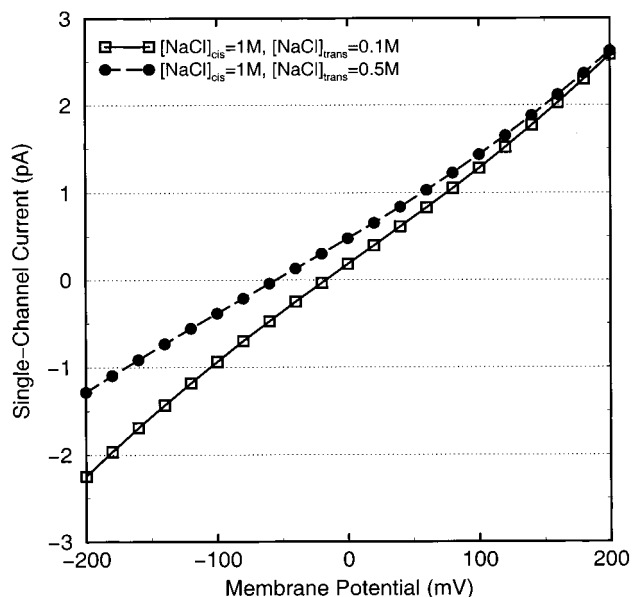(35) Wang, K.; Tripathi, S.; Hladky, S. B. *J. Membr. Biol.* **1995**, 247−257.

Figure 5. Predicted current−voltage relations for asymmetric NaCl salt solutions of 1 M vesus 0.1 M and 1 M versus 0.5 M. The open squares are for 1 M vesus 0.1 M, and the filled circles are for 1 M vesus 0.5 M NaCl solution.

1.46 to 1.88 pA. (The bathing solution was 1 M NaCl in this calculation, and the lipid dielectric constant was 2.) Although this result agrees with experimental estimates of the properties of water in the channel,[36] theoretical considerations[37,38] suggest that the dielectric properties of water inside the channel should be more complex.

Our calculations will be most useful if they predict (and thereby motivate) new experiments. Figure 5 predicts an unreported result, the $I-V$ relation of gA in asymmetrical solutions. The predicted current−voltage relation for 1 M||0.1 M is shown as the open squares, and that for 1 M||0.5 M is shown as filled circles, one representing a $10\times$ and the other a $2\times$ concentration gradient. A new experiment to confirm the calculation is being carried out, which we will report elsewhere.

Kurnikova et al. have recently shown that three-dimensional calculations of ions in channels are feasible and give reasonable results even if the surrounding solution is described by an artificial boundary condition.[18] The present work removes this boundary condition and provides new results: we predict the properties of channels embedded in macroscopic baths with neither adjustable parameters nor arbitrary boundary conditions. More generally, we show how the mathematically well-known method of spectral elements allows treatment of a macroscopic system (baths) and channel, with an emphasis in the channel pore region by putting finer elements (mesh) there. Furthermore, our present calculation uses one set of parameters in PNP theory to fit the $I-V$ values obtained in various ionic solutions. This calculation differs from that of Kurnikova et al. by assigning physically more reasonable diffusion coefficients to both sodium ion and chloride ions and by fitting the same experimental data via 1D PNP formulation. The present 3D formulation can be further used to study surface charge effect, since the entrance region of the channel pore opening is included explicitly.

In PNP theory, electrostatics is the only interaction of ions with the channel. No other specific interaction was included. Nonetheless, our 1D PNP study (to be published) of experimental data for both ion species shows that electrostatic interaction is enough to account for the different conductances between sodium ions and potassium ion. The difference in the values of diffusion coefficients (friction) for sodium ions and potassium ions and the same electrostatic interaction is enough to account for experimental data, without invoking other specific interaction. That is to say, if sodium ions are replaced with potassium ions in our calculation, the only change needed to fit the experiment is the value of the diffusion coefficient. Whether a specific interaction is needed to explain the data in the mixture of electrolyte solution remains to be investigated. One weakness in this continuum treatment is that the specific interaction of ions with water molecules is ignored, since water molecules are not treated explicitly. Water molecules are treated as a dielectric medium with a fixed dielectric constant in the bath and in the pore region of the channel. Volume exclusion of water molecules with ions and the ion solvation/dehydration effect need to be investigated further.

Conclusion

In summary, the electrodiffusion of sodium ions through gA can be predicted from the known structure of the channel using an empirical description of the charge on the atoms, if the prediction is made with spectral elements and a three-dimensional version of PNP. Our results suggest that electrostatics are a primary determinant of ionic movement through channels. It would be interesting to extend PNP to study other biological systems.

(36) Finkelstein, A.; Andersen, O. S. *J. Membr. Biol.* **1981**, *59*, 155.
(37) Duca, K.; Jordan, P. *Biophys. Chem.* **1997**, *65*, 123.
(38) Roux, B.; Prodhom, B.; Karplus, M. *Biophys. J.* **1995**, *68*, 876.